

INTERPRETATION OF SCHLUMBERGER SOUNDINGS  
AND HEAD-ON PROFILING

Mohammedberhan Abdulkadir,\*  
UNU Geothermal Training Programme  
National Energy Authority  
Grensasvegur 9, 108 Reykjavik  
ICELAND

\*Permanent address:  
Geological Survey of Ethiopia  
Geothermal Exploration Project  
P.O. Box 2302  
ETHIOPIA

ABSTRACT

The theory of resistivity measurements and the development of interpretation of vertical soundings is presented. In the early days of interpretation, mastercurves for different number of layers were established. These master curves were prepared for horizontally stratified earth. At present iterative methods which use the linear filter method are the most common. The advantage of the iterative methods is discussed.

Some theoretical apparent resistivities over two dimensional earth were computed and interpreted one-dimensionally to examine how inhomogenities affect the soundings.

Schlumberger soundings from the Corbetti caldera (Lakes District Rift, Ethiopia) were interpreted one and two-dimensionally. A resistivity map for the lowest resistivity between the depth of 200m and 1000m is presented. Low resistivity (5 Ohmm) was found to be along some geological features.

The theory and field procedure of the combined head-on resistivity profiling are discussed. The method was first introduced as a very useful tool in geothermal exploration by Cheng (1980). This method has been used, for the past few years, in Kenya and has been found to be useful in detecting faults and dykes (Mwangi, 1982). It has also been in use in Iceland for the past three years in combination with the modified Dey's program (Flovenz, 1984). Some theoretical curves for simple models are presented. These models were made to represent some simple geological features such as dykes, vertical contacts and dipping contacts. Head-on profiling data of one line from the Krafla high temperature geothermal field (Iceland) was interpreted as an example of the interpretation of head-on profiling.

TABLE OF CONTENTS

	Page
ABSTRACT .....	3
1 INTRODUCTION	
1.1 Scope of work .....	8
1.2 Introduction to resistivity survey .....	8
2 ONE-DIMENSIONAL INTERPRETATION	
2.1 Introduction .....	10
2.2 Development of interpretation of soundings .....	11
2.3 Computed resistivity .....	11
2.4 Sources of errors in Schlumberger soundings .....	13
3 TWO-DIMENSIONAL INTERPRETATION OF SCHLUMBERGER SOUNDINGS	
3.1 Introduction .....	15
3.2 Effect of lateral variation on vertical soundings ..	15
3.3 Theory of two-dimensional interpretation .....	16
4 INTERPRETATION OF SCHLUMBERGER SOUNDINGS FROM CORBETTI	
4.1 Introduction .....	20
4.2 Data quality .....	20
4.3 Geological setting .....	20
4.4 Results of interpretation .....	21
4.5 Discussion .....	22
5 HEAD-ON PROFILING	
5.1 Introduction .....	24
5.2 Field procedure .....	24
5.3 Principle of head-on profiling .....	25
5.4 Theoretical models .....	26
5.4.1 Vertical contacts .....	26
5.4.2 Dipping contact .....	27
5.4.3 Conduction dike .....	27
5.4.4 Conductive vertical block .....	27
5.5 Interpretation of head-on profiling .....	28
ACKNOWLEDGEMENTS .....	29
REFERENCES .....	30

APPENDIX I .....	44
<u>LIST OF FIGURES</u>	
2.1.1 Schlumberger array .....	32
2.4.1 Effect of near surface inhomogenties on Sc lumberger soundings .....	32
3.2.1 Two-dimensional model of soundings at different distance from a conductive dyke .....	32
3.2.2 Interpretation of sounding mesurements located at different distance from a conductive dyke .....	33
3.2.3 Two-dimensional model of a sounding located at the edge of a conductive dyke .....	33
3.2.4 Interpretation of a sounding located at the edge of the conductive dyke .....	33
4.4.1 Map of Corbetti caldera showing the location of the Schlumberger sounding stations .....	34
4.4.2 2-D model of line 40 .....	35
4.4.3 Measured and computed apparent resistivity pseudosections of line 40 .....	35
4.4.4 2-D model of line 43 .....	36
4.4.5 Measured and copmputed apparent resistivity pseudo-sections of line 43 .....	36
4.5.1 Resistivity map of Corbetti .....	37
5.2.1 Field lay out of head-on profiling .....	36
5.4.1 Head-on profiling over a vertical contact .....	38
5.4.2 Head-on profiling over dipping contacts .....	39
5.4.3 Head-on profiling over conductive dyke .....	40
5.4.4 Head-on profiling over conductive vertical block ....	41

5.5.1 Measured head on curves from Krafla (VS3) .....	42
5.5.2 Model of VS3 .....	42
5.5.3 Computed curves of the model VS3 .....	43

## 1 INTRODUCTION

### 1.1 Scope of work

This report is a part of the author's work during six months geothermal training in Iceland under the sponsorship of the United Nations University and the Icelandic Government, from April to October 1984.

The training started by 4 weeks of introductory lectures which covered planning, exploration, drilling, utilization and environmental impact of geothermal energy. The author received practical training in head-on profiling, Schlumberger soundings, magnetic and gravity data collection. This was followed by one week field excursion in which the author visited various sites, power stations, industries, schools and farms which utilize geothermal energy. The author also participated in geological field work where he got the orientation of how geological and geophysical exploration go hand in hand.

The rest of the training time was devoted to the study of the theory of interpretation of Schlumberger soundings and practical training in the interpretation of Schlumberger soundings and head-on profiling.

### 1.2 Introduction to resistivity survey

The main reason why resistivity surveys are of a great importance in geothermal exploration is the nature of the thermal water to change its electrical resistivity with change in temperature.

Resistivity decreases with increasing temperature up to 300°C, but increases with higher temperature. The resistivity can also decrease because of the assemblage of conductive minerals in microfissures in the rocks. This usually indicates the presence of thermal fluid.

The detection of dykes and faults with resistivity surveys is another important property which makes these surveys suitable in geothermal exploration.

The main problem in these surveys is the effect of faults and dykes on the soundings, which has been minimized recently with two dimensional interpretation of soundings where the effect is significant. Dey and Morrison (1976) have developed a mathematical formulation for two dimensional earth and in the same year Dey wrote a two-dimensional computer program for computing apparent resistivities for two-dimensional model. This program (Dey, 1976) was used during the author's training.

Despite the importance and development mentioned above resistivity surveys have certain limitations. They enable location of low or high resistivity areas, but which of the detected electrical structures are promising from the geothermal point of view needs a good agreement of all the scientific surveys made in the area.

## 2 ONE DIMENSIONAL INTERPRETATION

### 2.1 Introduction

For homogenous and isotropic earth the potential  $V$  due to a point source on the surface is given by:

$$V = \frac{\rho I}{2\pi r} \quad (2.1.1)$$

Where  $\rho$  is the resistivity,  $r$  the distance between the point source and  $I$  is the current injected through the point source.

It can easily be seen from (2.1.1) and Fig 2.1.1 that the potential difference between two points  $M$  and  $N$  due to two point sources  $A$  and  $B$  with current  $+I$  and  $-I$  respectively is given by:

$$\Delta V = \frac{\rho I}{2\pi} \left( \frac{1}{AM} - \frac{1}{AN} - \frac{1}{BM} + \frac{1}{BN} \right) \quad (2.1.2)$$

Solving for resistivity:

$$\rho = 2\pi \cdot \frac{\Delta V}{I} \cdot \left( \frac{1}{AM} - \frac{1}{AN} - \frac{1}{BM} + \frac{1}{BN} \right)^{-1} \quad (2.1.3)$$

For Schlumberger array, a colinear array where the separation between the potential electrodes is very much smaller than that of the current electrodes (i.e.  $MN \ll AB$ ), equation (2.1.3) can be rewritten as:

$$\rho = \frac{\pi}{4} \cdot \left( \frac{(AB)^2}{MN} - MN \right) \cdot \frac{\Delta V}{I} \quad (2.1.4)$$

The resistivity  $\rho$  can be found by injecting current  $I$  through one electrode and completing the circuit by another electrode and measuring the resulting potential difference between two points of observation. The resistivity observed by this method is not the true resistivity of the earth, because both of the above equations are true if and only if the earth is homogeneous, but in reality the earth is nowhere homogeneous. Therefore the resistivity which we



obtain from the measurements with the help of equation (2.1.4) is referred to as apparent resistivity and usually denoted by  $\rho_a$ .

The idea of interpretation is to find a model of resistivity layers (or structures) reproducing apparent resistivities which fit the observed ones.

## 2.2 Development of interpretation of soundings

The history of the interpretation of vertical electrical soundings goes as far back as the application of resistivity surveys. In the early days of interpretation, mastercurves of apparent resistivity were used extensively.

Tank models were also used to a very limited extent. The limitation of the tank model curves is that no solution homogeneous enough exists. And moreover, it is not possible to construct the tanks in such a way that they do not affect the results.

At present iterative methods which use the linear filter methods are extensively in use. The approach to these methods is discussed in the next section.

## 2.3 Computed resistivity

Assuming that the earth is made up of horizontally stratified layers and that each layer is electrically homogeneous and isotropic it can be shown that the Laplacian of the potential due to a point source on a surface is equal to zero.

$$\nabla^2 V = 0 \quad (2.3.1)$$

An equation for potential  $V$  can be derived from (2.3.1) (Koefoed, 1979)

$$V = \frac{\rho I}{2\pi} \int_0^{\infty} [1 + 2\theta_1(\lambda)] J_0(\lambda r) d\lambda \quad (2.3.2)$$

Where  $I$  is the current intensity;  $\rho_1$  is the resistivity of the first layer;  $\lambda$  is the variable of integration;  $r$  is the distance from the current source to the measuring point;  $j_0$  is a Bessel function of zero order;  $\theta_1(\lambda)$  is a Kernel function which is controlled by the resistivities of the layers.

The apparent resistivity for the Schlumberger array can be calculated by substituting the potential difference calculated from (2.1.3) into (2.3.2).

$$\rho_a = \left(\frac{AB}{2}\right)^2 \int_0^{\infty} K(\lambda) J_1(\lambda AB) \lambda d\lambda \quad (2.3.3.)$$

Most of the modelcurves were established by numerical integration of equation (2.3.3) for different number of layers.

The linear filter method which was first introduced by Gosh (1971) is the one most widely used today.

For the Schlumberger arrangement

$$\rho_a = \left(\frac{AB}{2}\right)^2 \int_0^{\infty} T_1(\lambda) J_1(\lambda AB) \lambda d\lambda \quad (2.3.4)$$

Where  $T_1(\lambda)$  is the resistivity transform (Koefoed, 1979; Gosh, 1971).

The idea behind this method is to calculate the resistivity transform for a given model and obtain a calculated resistivity using equation (2.3.4). Then by trial-and-error method the model (thickness and resistivity) is changed until the best fit of the calculated and observed resistivity is obtained. The trial-and error method can be carried out by an iterative least-square method.

In the indirect methods, there exist infinitely many models which reproduce the measured data. Oldenburg (1978) has shown that the non-uniqueness can be resolved by determin-

ing only averages at each depth. All resistivity structures which are linearly close to the constructed model will have the same averages.

ELLIPSE is a program for one dimensional interpretation of Schlumberger soundings written by Ragnar Sigurdsson (Orkustofnun, Iceland). It is based on an automatic iterative method, facilitated by the linear filter method. It has advantages over many other programs in that it takes into account the potential differences at different separations of potential electrodes for the neighbouring current electrode separations. Moreover, the program takes into consideration the standard deviation and number of readings of the potential differences in determining the averages of each data point. ELLIPSE was used during the training of the author.

#### 2.4 Sources of errors in Schlumberger soundings

It is well known that the inaccuracies of the field measurements in D.C resistivity soundings of order of 3% make an interpretation in terms of resistivity and thickness rather ambiguous (Johanson, 1977). Thus we have to minimize the source of errors for better interpretation. Some of the main source of errors and possible solutions are discussed below.

Instrumentation: Erroneous readings usually occur due to low internal resistance of the potential measuring instruments. If the internal resistance of the instrument is too low, there will be a tendency of diversion of current from its flow because the potential circuit acts as a parallel circuit.

This problem can be tackled by using receivers of a very high internal resistance. In Iceland (Orkustofnun) a homemade (by the firm Microprocessors) receiver of a very high impedance (of 100 mega-ohm) is used in all the resistivity surveys. This receiver has also some other capabilities that many commercially produced receivers do not have. It is stimulated by the transmitter to start reading as the potential difference does not reach it's

final value as soon as the polarity of current is reversed. It also displays the standard deviation and the number of readings which enables the operator to control his data collection and can be used later in the interpretation.

**Leakage:** If current leaks from the current circuit to the potential circuit the potential difference will be distorted, which could be interpreted as a two dimensional effect. Therefore it is advisable to check the wires regularly, for example by transmitting current while the circuit is disconnected and measuring the resulting potential which should be zero if there is no leakage.

**Topography:** Current density is very much affected by topography. It is high in depressions and low at higher altitudes. Thus if the potential electrodes are situated at different elevations the measured potential will be distorted. This problem can be solved by selecting the stations in such a way that the potential electrodes will be situated in a flat terrain.

**Near surface inhomogenities:** A disturbed curve can be obtained if the potential electrodes are situated on surfaces with different resistivities. This problem can be tackled by taking many measurements with different potential electrode separations for each current electrode separation.

It can be noted from Fig 2.4.1 how the curve would look like if the potential electrodes were moved (broken line) without taking measurements for overlaps. This type of shift can also be obtained due to eccentricity.

### 3 TWO-DIMENSIONAL INTERPRETATION OF SCHLUMBERGER SOUNDINGS

#### 3.1 Introduction

In one-dimensional interpretation it is assumed that each layer is electrically homogeneous. This assumption practically holds true if the contrast of resistivities of the geological structures within that layer is not too large. But where there are very conductive or resistive dykes or faults, which is common in geothermal areas, the effect on the sounding is very significant. Many attempts were made to solve this problem by the image method. Van Nostrand and Cook (1955), De Gery and Kuntez (1955) have published mastercurves over simple structures by the image method.

#### 3.2 Effect of lateral variation on vertical soundings

In the case where there are dykes and faults (or any medium with very large contrast) there will be a distortion in distribution of the current density.

In Fig (3.2.1) locations of soundings ( $S_1$  and  $S_2$ ) are shown. The apparent resistivities for these soundings were calculated with Dey's program (a program for two dimensional interpretation). The corresponding potential difference for each apparent resistivity was computed and the soundings were interpreted with ELLIPSE  $S_1$  and  $S_2$  were stationed on two layered earth, at 100 m and 1000 m from a vertical dyke respectively. The model obtained with one-dimensional interpretation was different from the model given in Fig (3.2.1). The computed apparent resistivities are given in Appendix I. The interpretation results of both soundings are given in Fig (3.2.2).

The response of the sounding located at the edge of the conductive dyke (Fig 3.2.3) was calculated using Dey's program. The computed apparent resistivities are given in Appendix II. These apparent resistivities were interpreted in one dimension using the same procedure as in the case of  $S_1$  and  $S_2$ . The model obtained from this interpretation was different from the original two dimensional model which reproduced the apparent resistivities.

From the discussion above it can be concluded that in one dimensional interpretations careful attention must be paid if neighboring soundings are dissimilar. And where the curves are similar in the case of soundings  $S_1$  and  $S_2$  there is hardly any way to recognize whether a curve is affected by a two dimensional structure or not. But the use of overlaps discussed in section (2.4) can be of a great help. The case where the slope exceeds one is of course trivial if all sources of errors are minimized.

Low resistivity areas, in geothermal fields, may occur due to high resistivity contrast of faults. But low resistivity area along a fault can also occur if the thermal fluid is flowing along the fault. Thus, to find out what causes the low resistivity, two-dimensional interpretation must be practiced where ever two-dimensional effect is indicated.

### 3.3 Theory of two dimensional interpretation

Dey and Morrison (1976) have developed a numerical technique, to solve three-dimensional potential distribution from a point source located in or on the surface of a half space containing arbitrary two-dimensional conductivity distribution.

The current density  $J$  is related to the electric field intensity  $E$  and an isotropic conductivity  $\sigma$  by Ohm's law i.e.

$$\vec{J} = \sigma \cdot \vec{E} \quad (3.4.1)$$

Since the stationary electric fields are conservative,

$$\vec{J} = -\sigma \nabla V \quad (3.4.2)$$

Applying the principle of conservation of charge over volume, using the equation of continuity:

$$\nabla \cdot \vec{J} = \frac{\partial \rho}{\partial t} \delta(x)\delta(y)\delta(z) \quad (3.4.3)$$

Where  $q$  is the charge density specified at a point in the cartesian X-Y-Z space by the Dirac delta function.

Equation (3.4.3) can be rewritten for a generalized three dimensional space as:

$$\nabla \cdot [\sigma(x,y,z) \bar{\nabla} V(x,y,z)] = \frac{\partial q}{\partial t} \delta(x_s) \delta(y_s) \delta(z_s) \quad (3.4.4)$$

Where  $(X_s, Y_s, Z_s)$  indicates the coordinates of the point source of charge injected in the X-Y-Z space.

Equation (3.4.4) can be rewritten as

$$\bar{\nabla} \sigma(x,y,z) \bar{\nabla} V(x,y,z) + \sigma(x,y,z) \nabla^2 V(x,y,z) = - \frac{\partial q}{\partial t} \delta(x_s) \delta(y_s) \delta(z_s) \quad (3.4.5)$$

Assuming that the conductivity in Y-direction is constant, equations (3.4.4) and (3.4.5) can be rewritten as:

$$-\bar{\nabla} \cdot [\sigma(x,z) \bar{\nabla} V(x,y,z)] = \frac{\partial q}{\partial t} \delta(x_s) \delta(y_s) \delta(z_s) \quad (3.4.6)$$

and

$$\bar{\nabla} \sigma(x,z) \cdot \bar{\nabla} V(x,y,z) + \sigma(x,z) \nabla^2 V(x,y,z) = - \frac{\partial q}{\partial t} \delta(x_s) \delta(y_s) \delta(z_s) \quad (3.4.7)$$

Equation (3.7.4) can be rewritten as:

$$\begin{aligned} & \nabla^2 [\sigma(x,z) V(x,y,z)] + \sigma(x,z) \nabla^2 V(x,y,z) - V(x,y,z) \nabla^2 \sigma(x,z) \\ & = - 2 \frac{\partial q}{\partial t} \delta(x_s) \delta(y_s) \delta(z_s) \end{aligned} \quad (3.4.8)$$

In the last two equations, the conductivity is a function of  $x$  and  $z$  and the potential and the source term are functions of  $x$ ,  $y$  and  $z$ . For simplicity it is preferable to solve these equations in Fourier transformed space  $(x, K_y, z)$  by transforming  $y$  into  $K_y$  domain.

By performing forward transformation, the three dimensional potential distribution  $V(x, y, z)$  due to a point source at  $(x_s, y_s, z_s)$  over two dimensional conductivity distribution  $\sigma(x, z)$  is reduced to the two-dimensional transformed potential  $V'(x, K_y, z)$  which is a solution of the transformed equation (3.4.6).

$$-\vec{\nabla} \cdot [\sigma(x, z) \vec{\nabla} V'(x, k_y, z)] + K_y^2 \sigma(x, z) V'(x, k_y, z) = Q \delta(x_s) \delta(z_s) \quad (3.4.9)$$

and similarly a solution for (3.4.8) is given by:

$$\begin{aligned} \nabla^2 [\sigma(x, z) V'(x, k_y, z)] + \sigma(x, z) \nabla^2 V'(x, k_y, z) - V'(x, k_y, z) \nabla^2 \sigma(x, z) \\ - 2K_y^2 \sigma(x, z) V'(x, K_y, z) = - 2Q \delta(x_s) \delta(z_s) \end{aligned} \quad (3.4.10)$$

for a fixed value of  $K_y$  the parameter  $Q$  defined in the above equations is the constant steady state current in  $(x, K_y, z)$  space, given by:

$$Q \delta(x_s) \delta(y_s) = \frac{I}{2} \cdot \frac{\partial q}{\partial t} \delta(x_s) \delta(z_s) \quad (3.4.11)$$

The current density  $Q$  can be related to the current  $I$  injected at  $(x_s, z_s)$  by:

$$Q = \frac{I}{2\Delta A} \quad (3.4.12)$$

Where  $\Delta A$  is a representative area in  $x$ - $z$  plane about the injected  $(x_s, z_s)$ .

Dey and Morrison (1976) obtained numerical solution to equation (3.4.9) and (3.4.10) subject to the continuity boundary conditions. These boundary conditions are:

- (i)  $V(x, y, z)$  must be continuous across each boundary of the physical property distribution of  $\sigma(x, z)$ .
- (ii) the normal component of  $J$  must be continuous across each boundary.



The solution of  $V'(x, K_y, z)$  is obtained by deriving the "difference equations" of (3.4.9) and (3.4.10), by proper discretization of the  $(x, K_y, z)$  space over which the problem is to be solved. This numerical technique is used to solve the primary potential due to the point source and the perturbational potential due to the conductivity of inhomogeneties at each node of discretized half space. Dey (1976) wrote a FORTRAN algorithm named RESIS2D to implement such a generalized method. This program calculates potential response of two-dimensional geological bodies of any shape.

The two-dimensional interpretation is carried out by constructing a model of vertical blocks of different layers and computing the response with the program. The computed apparent resistivities are then compared with the observed ones manually and the trial and error method continues until the best fit is obtained.

In this interpretation, as well as in one-dimensional interpretation, there are infinitely many models which reproduce the observed apparent resistivities. Thus, correlation between one and two-dimensional interpretation must be made. In fact, inferring the initial model from one-dimensional interpretation for the part of the curve, which is not affected two-dimensionally, will be of a great help in two-dimensional interpretation.

## 4 INTERPRETATION OF SCHLUMBERGER SOUNDINGS FROM CORBETTI

### 4.1 Introduction

Some Schlumberger soundings from Corbetti geothermal field (LAKES DISTRICT RIFT, ETHIOPIA) were interpreted. The data were collected between March 1983 and February 1984. Most of the data had previously been interpreted and presented in Corbetti Geophysical Report I (Befekadu, et al., 1983), but in the present report the interpretation was carried out with much better automatic iterative program. Moreover two lines were interpreted two-dimensionally. Hence a better resistivity map of the area is presented.

In this survey IPR10 and IPR10A receivers and 15 and 2.5 KW transmitters were used. The frequency used was 0.125 HZ (T = 2sec, nearly square pulse).

### 4.2 Data quality

Despite the rugged topography the data collected generally gave good information. An effort was made to minimize all sources of errors. However, two problems arose as only few data points were taken in the first decades (i.e for  $AB/2 < 100$  m) and overlaps were practiced for  $AB/2 > 70$  m. These problems made interpretation with ELLIPSE difficult. Therefore modifications were made in the interpretation of each sounding.

### 4.3 Geological setting

The Corbetti caldera is located in the lowest part of the Ethiopian rift system between lake Awasa and lake Shalla. The caldera is elliptical and its elongation (E-W) is related to the main tectonic trend of the Ethiopian rift. The diameter of the caldera is 10-18 km (Elias, 1983).

The Corbetti caldera is formed exclusively by volcanic products. Most of the volcanic products which outcrop in this area and in the entire Ethiopian Rift Valley, are

related to fissure eruptions. The recent basaltic lavas are located along the active faults of the valley. (Di Pola, 1972)

"Most probably the eruption of such impressive amount of pyroclastic material produced a regional collapse which originated the Corbetti caldera. Even the two recent volcanoes, Urji and Chebi, grown inside the Corbetti caldera, are related to the still active tectonic lines of the floor of the Rift valley." (Di Pola 1972)

Hydrothermal manifestations in Chebi volcano have higher temperature (96°C) than those of Urji and Danshe volcanoes. In most of the area of thermal manifestations, the pumice is cemented by silica and acts as impermeable layer (Elias 1983).

#### 4.4 Results of interpretation

The location of the soundings is shown in Fig (4.4.1). The model and the results of the one-dimensional interpretation are presented in Appendix III.

Soundings taken on line 40 were affected two-dimensionally. This was observed on  $AB/2 > 1470$  m in most of the soundings (Figs. 4.4.2, 4.4.3). The effect (slope greater than one) on the soundings inside Borena, which is a crater on the eastern rim of the caldera, the effect is observed for  $70\text{m} < AB/2 < 215\text{m}$ . Many types of block arrangements were tried between stations 5.0 and 6.0 but with no success, which probably indicates that the effect in this particular area is three-dimensional. This suggestion is supported by the fact that station 5.0 is located near the caldera rim to the south and the crater rim to the east. Generally all soundings which were located inside Borena show low apparent resistivities in the upper layer and relatively higher at the middle and the same sequence in the lower layers. The higher resistivity below the surface resistivity seems to be due to high resistivity at the rim of the crater as can be seen by the increase of the apparent resistivities immediately after the current electrodes cross the rim. Hence it is reasonable to put a block of

relatively higher resistivity at the rim of the crater. Addition of a high resistivity block between station 5.0 and 6.0 can, however, be misleading. Therefore these stations were omitted in the interpretation and the northern part of the line was interpreted two-dimensionally. The two stations (7.0 and 8.0) on the southern part of the line were interpreted one-dimensionally with good accuracy. From the two-dimensional model Fig (4.4.1) and the model for one-dimensional interpretation in Appendix I it can be noted that the low resistivity is confined to the central part of the line which coincides with the central part of the crater.

Line 41 was interpreted one-dimensionally with a good accuracy except in the station located in Borena. Lines 42 and 44 were also interpreted one-dimensionally with very good accuracy.

Line 43 was interpreted both one and two-dimensionally (Fig. 4.4.4, 4.4.5) and some differences were observed in the central part of the line at the boundary between low and relatively higher resistivity occurs.

Some soundings which were not on line, purposely made to control the extrapolation on a rugged terrain with the best suitable orientations, were interpreted successfully.

#### 4.5 Discussion

A resistivity map was made (Fig 4.5.1) from the results of the interpretation. The map is made for the lowest resistivity within a depth of 200-1000 m. The low resistivity (less than 5 Ohmm) follows some geological features. This low resistivity covers the south-eastern part of Chebi follows the eastern caldera rim northwards and through Borena towards west and continues until it changes direction which seems to be controlled by another geological feature towards north. Using the dipole-dipole interpretation from the Corbetti report (Befekadu, et al., 1983) the low resistivity continues northwards where it increases to 10 ohmm and broadens on the southern shore of lake Shalla.

The results shown on the map should not be overlooked, even though the map was made with results of only few stations in particular where X10 is located and the cause of the low resistivity is not yet well defined. But as far as the interpretation of the soundings is concerned it seems likely that the thermal fluid is controlled by the caldera wall, the crater and the faults.

The presence of hot springs on the southern shore of Lake Shalla and the absence of any thermal manifestation between the northern shore of lake Awasa and the southern rim of the caldera, may lead to the conclusion that the heat is situated within the caldera and the sink is Lake Shalla. Other supporting evidence for this argument is the low temperature in the Wondo-Kosha borhole (south of the caldera) and relatively higher temperature in the boreholes around Aje (north-west of the caldera). Based on these facts the obtained results of the resistivity survey look very reasonable and encourage further survey of the low resistivity area. Therefore the author would like to recommend:

1. Additional soundings or other resistivity surveys on areas where there are only few stations, in particular between Jama Humo and Danshe, between Jama Chebi and Jama Humo and around station X10 in order to obtain better extrapolation.
2. Head-on survey along line 40 must be tried from station 2.5 as far south as possible. Head-on profiling survey perpendicular to the low resistivity structure on the western side is recommended to delineate the location of the geological structure which controls the low resistivity zone on the western side of the caldera.

## 5 HEAD-ON PROFILING

### 5.1 Introduction

The "combined, head-on resistivity profiling method" was first developed in 1958 in China to detect narrow, conductive zones in mining and hydrological prospects. It was first introduced in geothermal prospecting as an important means of detecting faults and dykes by Cheng (1980).

This method has been in use for the past three years in Iceland and found to be a very useful tool in detecting concealed faults and dykes along which the thermal fluid ascends to the surface, (specially in low enthalpy geothermal systems) (Flovenz, 1984). It is also being practiced in high enthalpy geothermal system (Krafla) in correlation with other resistivity methods. The facility of interpretation with the modified Dey's program is another encouraging factor which causes the head-on method to be used extensively in Iceland.

It has also been used in Kenya for the past few years and has shown positive results (Mwangi, 1982).

### 5.2 Field procedure

The main difference between the classical Schlumberger method and head-on profiling is that there is one additional current electrode at infinity. Basically the potential difference in the potential circuit is supposed to be only due to the current injected by one electrode since one electrode is situated at infinity. The field procedure is shown in Fig (5.2.1). C is the location of the additional current electrode.

Measurements of the potential differences are made for current injected through A and the circuit made complete at C, an electrode at infinity, and similar procedure for the current injected through B. Measurements are also taken for current injected through A and B which will help as a check

for the separate measurements. The procedure is repeated for many stations along a line with very short distance between neighboring stations (preferably 25 m).

The data is presented by plotting  $\rho(AC) - \rho(AB)$  and  $\rho(BC) - \rho(AB)$  for a fixed  $AB/2$  for each station on a line.

### 5.3 Principle of head-on profiling

The basic principle of head-on profiling lies in the theory of potential distribution in the different geological structures with different resistivity in the vicinity of the electric field due to the current electrode. As mentioned in Chapter 3, the current density which is related to the resistivity by Ohm's law is very much affected by structures with large contrast of resistivity. Therefore the measured potential depends on the conductivity of the geological structure, dimension, and distance between the structure which causes inhomogeneity and the current and potential electrodes.

The relation between  $\rho(AB)$  and that of the  $\rho(AC)$  and  $\rho(BC)$  is given below.

$$\rho(AB) = \frac{2\pi\Delta V}{I} \cdot \left( \frac{1}{AM} - \frac{1}{AN} - \frac{1}{BM} + \frac{1}{BN} \right)^{-1} \quad (5.3.1)$$

$$\rho(AC) = \frac{2\pi\Delta V}{I} \cdot \left( \frac{1}{AM} - \frac{1}{AN} - \frac{1}{CM} + \frac{1}{CN} \right)^{-1} \quad (5.3.2)$$

$$\rho(BC) = \frac{2\pi\Delta V}{I} \cdot \left( \frac{1}{BN} - \frac{1}{BM} - \frac{1}{CN} + \frac{1}{CM} \right)^{-1} \quad (5.3.3)$$

As C is assumed to be situated at infinity the reciprocals involving C will converge to zero. Under this condition the geometric factor in (5.3.1) is equal to the sum of the geometric factors in (5.3.2) and (5.3.3). Therefore the relationship between the three equations is reflected in the relation between  $\Delta V$ ,  $\Delta V'$  and  $\Delta V''$ . The differences are caused by perturbed potential due to inhomogeneities. For

example, if there is a conductive medium between current electrode A and the observation, more current will flow in the conductive medium if current is injected through A and lower potential will be observed. And if current is injected through B the current density will be high near the potential electrode which means higher potential if the potential electrode is near the inhomogeneity. The potential due to A and B will contain both effects. Hence it can be concluded that  $\Delta V$  is equal to the sum of  $\Delta V'$  and  $\Delta V''$ . Obviously in the case where there is no inhomogeneity  $\Delta V'$  and  $\Delta V''$  will be equal.

#### 5.4 Theoretical models

Some theoretical model curves computed with the modified Dey's program are presented in this section. These models are selected such that they give information on how the curve would look like for different geological structures. In particular it is discussed under what conditions cross-over occurs and under what conditions the curve converges or diverges.

##### 5.4.1 Vertical contacts

The curve in Fig 5.4.1 shows that the curve for measurements perpendicular to a fault of high resistivity diverges over the vertical contacts. The resistivities of all the three cases were equal before the current electrode B approached the fault. But as soon as it was on the resistive medium  $\rho(AB)$  began to increase, and  $\rho(AC)$  and  $\rho(BC)$  began to diverge. When the array was some distance away from the contact the differences tended to diminish again.

It can also be noted from the difference between Fig 5.4.1 (a) and (b) that the distance between the electrode and the contact plays an important role. For  $AB/2 = 250$  m and 500 m the abrupt change occurs respectively at 250 m and 500 m from the contact.



#### 5.4.2 Dipping contact

Fig 5.4.2a shows a curve of measurements over a dipping contact (a dip of  $11^\circ$ ). The curve diverges at about 70 m distance in the same way as the curve over a vertical contact does (Fig 5.4.1).

Similar divergence was obtained for a contact with  $45^\circ$  dip (Fig 5.4.2b). From this it seems that dipping contacts can be misinterpreted as vertical contacts displaced from their exact location. Thus it is advisable to correlate the interpretation obtained from soundings with the modelling of the head-on survey.

#### 5.4.3 Conductive dyke

Fig 5.4.3 shows a curve for head-on profiling over a conductive vertical dyke. As shown in the Figure the cross-over occurs at the middle of the dyke. This indicates that the potential distribution due to the heading and the lagging current electrodes was equal. If the dyke was highly resistive the cross-over would occur but the plot for  $\rho(AC-AB)$  and  $\rho(BC-AB)$  would be reversed.

#### 5.4.4 Conductive vertical block

On Fig 5.4.4 a curve for a 600 m wide conductive vertical block situated in a homogeneous resistive medium is shown. For the stations in the neighborhood of 0 the whole array is within the conductive region, but still the cross-over appears. The same explanation holds true for a resistive block.

From this discussion it can be concluded that any medium with high contrast of resistivity to its sides will cause cross-over on the  $\rho(AC-AB)$  and  $\rho(BC-AB)$  curves. In the case where there are two similar structures of the same resistivity on both sides of the station no cross-over will appear because the effect will be cancelled.

### 5.5 Interpretation of a head-on profile from Krafla

In 1983 head-on profiling survey was carried out in the Krafla high temperature geothermal field. The objective of the survey was to find out the cause of the low resistive area which was very difficult to locate with soundings due to high variation in lateral resistivities. The aim of the interpretation in this section is not to give complete analysis of the survey, but to discuss how to carry out the interpretation in the real earth.

The data was collected for three current electrode separations ( $AB/2 = 750$  m, 500 m and 250 m) and for fixed potential electrode separation ( $MN/2 = 25$  m).

The initial model was inferred from the one-dimensional interpretations of the soundings on the line and from qualitative analysis of the head-on data. In one of the soundings located in the middle (KR-106) a very high jump was observed. In the interpretation a low resistivity of 4.4 ohmm at a depth of about 760 m was obtained (Krafla-Hvitholar, 1983). The thickness of this low resistivity layer was 1312 m, whereas the maximum  $AB/2$  was only 1580 m. This indicates that the low resistivity layer is the bottom layer. The additional layer might be due to the complexity of the geological structure of the area. At the location of this sounding cross-overs were observed in the head-on data for all the three current electrode separations. The cross-over was due to low resistivity vertical block, as can be seen from the observed curves in Fig (5.5.1). There was also a cross-over at about 700 m to the left of the mentioned low resistive block for  $AB/2 = 500$  m. The cross-over in this case was due to high resistivity structure. An initial model was constructed from this qualitative analysis. The penetration depth was assumed to be about  $AB/4$ . However, it was discovered that the penetration depth was less than  $AB/5$ . This was observed from the fact that the changes made for 500m under the previous assumption affects the 750 m separation. Therefore later models were constructed for penetration depth less than  $AB/5$ . The model is given in Fig 5.5.2 and the computed

curves in Fig 5.5.3. The resistivities in the lower layers of all the blocks have no effect on the computed curves but were made to match the one-dimensional interpretation.

#### ACKNOWLEDGMENTS

I wish to acknowledge the organizers of the Geothermal Training Programme for granting me this fellowship. I am deeply indebted to Brynjolfur Eyjolfsson for his supervision and advice during the training. I would like to thank Ingvar B. Fridleifsson for his valuable advice and reading the manuscript.

My thanks are to all lecturers of the programme, Ragnar Sigurdsson for the explanation of the program he wrote and Sigmundur Einarsson for valuable explanation on the approach to geological field work in geothermal areas.

My special thanks are to Sigurjon Asbjornsson who took care of us during our stay in Iceland.

I would like to acknowledge the Ethiopian Geothermal Exploration geophysics field crews for their great effort in the data collection and Befekadu Oluma and Abiy Hunegnaw during their supervision in the geophysical survey of the Corbetti area.

Thanks to the United Nations University fellows of the 1984 for good time together.

REFERENCES

Befekadu, Abiy and Mohammedberhan, 1983: Geophysical Exploration of Corbetti report I, Geothermal Exploration Project (lakes District Rift, Ethiopia).

Cheng, Y.W., 1980: Location of nearsurface faults in geothermal prospects by "Combined head-on Resistivity Profiling method", Proceedings of the New Zealand Geothermal Workshop, 1980, 163-166.

Dey, A., 1976: Resistivity Modelling for Arbitrarily Shaped Two Dimensional Structures Part II: User's Guide to the FORTRAN Algorithm RESIS2D. LBL 5283.

Dey, A. and Morrison, 1976: Resistivity Modeling for Arbitrarily Shaped Two Dimensional Structures, Part I: Theoretical Formulation. LBL 5223

DeGerg J.C. and Kunetz, G., 1956; Potential and resistivity over dipping beds, Geophysics 21, 780-793.

DiPola, 1972; Geology of the Corbetti Caldera Area . (Main ETHIOPIAN Rift Valley). Reprinted from Bulletin Volcanologique, Tome XXXV-2, 1972, 497-506.

Elias, 1983: Preliminary Report of Geology and Thermal Manifestations of Corbetti Volcano, Geothermal Exploration Project (Lakes District Rift, Ethiopia).

Flovenz, O., 1984: Application of the head-on Resistivity profiling Method in Geothermal Exploration, Geothermal Resources Council Transactions vol. 8.

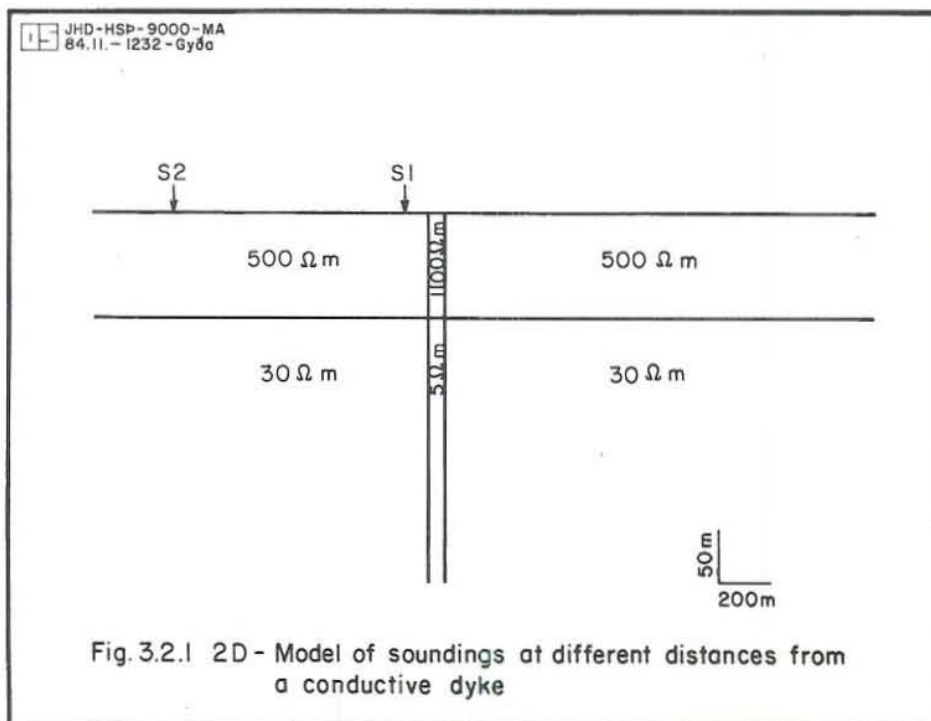
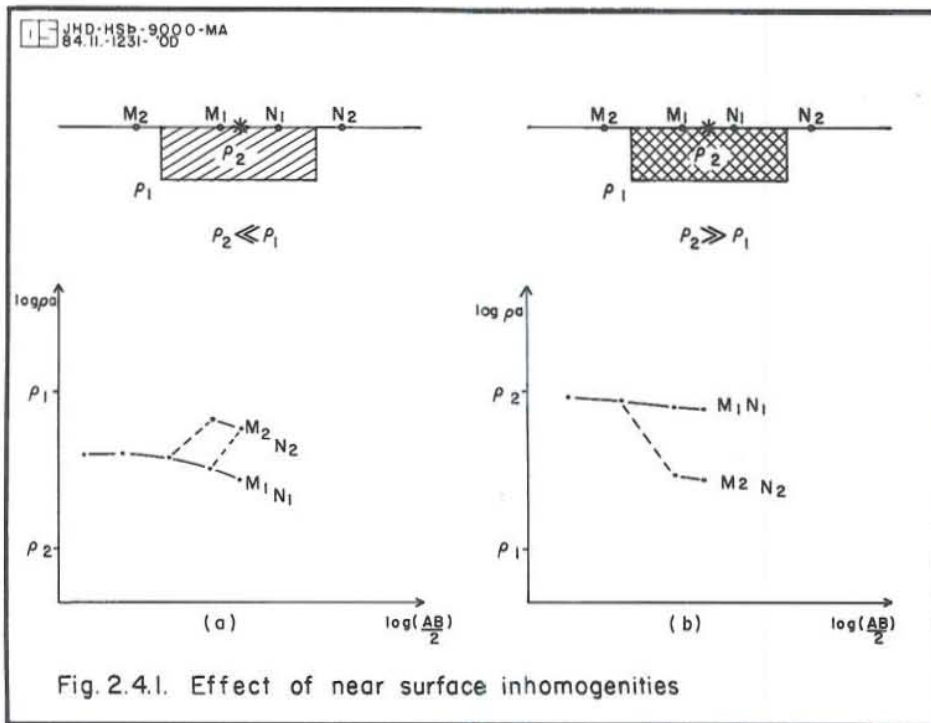
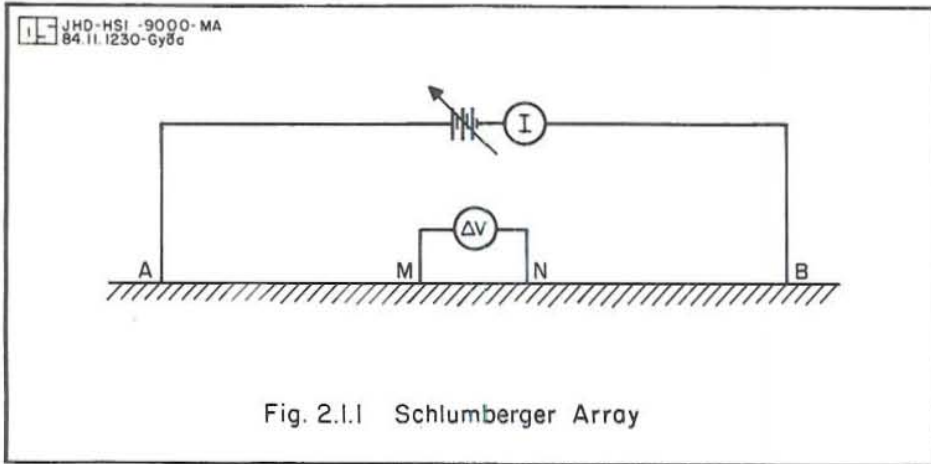
Johanson, H.K, 1977: A Man/Computer Interpretation System for Resistivity Soundings over a Horizontally Stratified Earth, Geophysical Prospecting 25, 667-691.

Koefoed, O., 1979: Resistivity Soundings on an Earth Model Containing Transition Layers With Linear Change of Resistivity with Depth, Geophysical Prospecting 27, 862-868.

Mwangi, M., 1982: Two dimensional Interpretation of Schlumberger Soundings and Head-on Data ,UNU Geothermal Training Programme, report 1982-9.

Oldenburg, D.W., 1978; The Interpretation of Direct Current Resistivity Measurements Geophysics, Vol. 43. No.3, 1978, 610-625.

VanNostrand, R.G. and Cook, K.L., 1955; Apparent resistivity for dipping beds - a discussion, Geophysics, 20, 140-147.



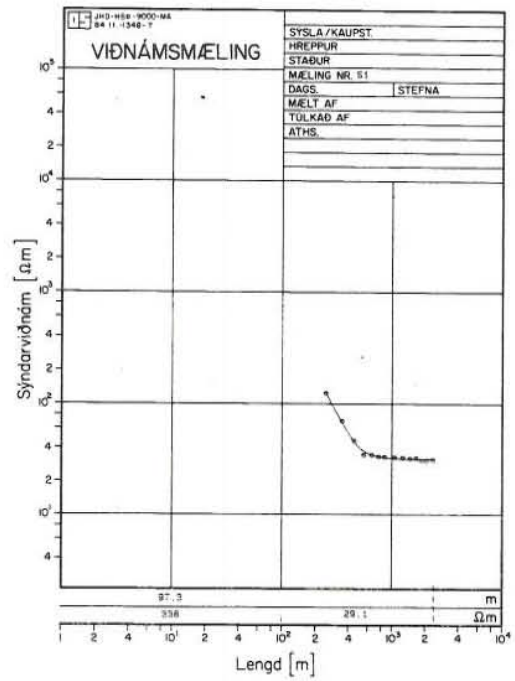
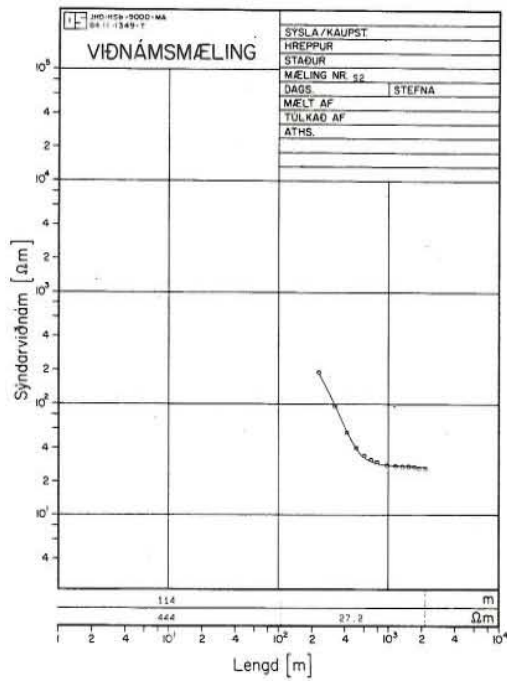


Fig. 3.2.2 Interpretation of sounding measurements located at different distance from a conductive dyke.

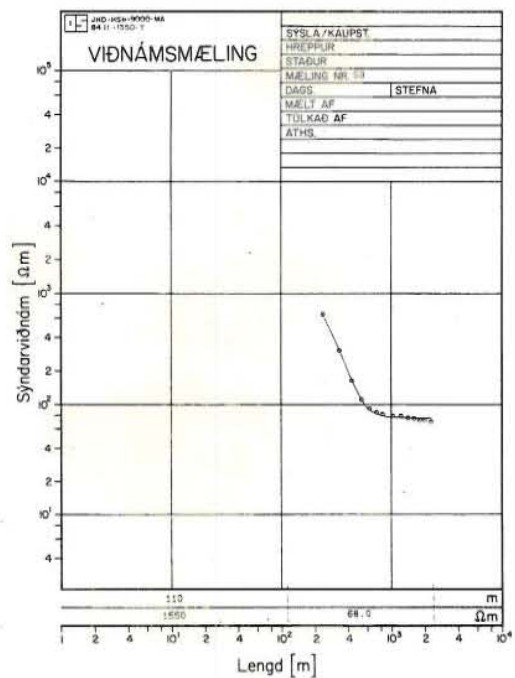
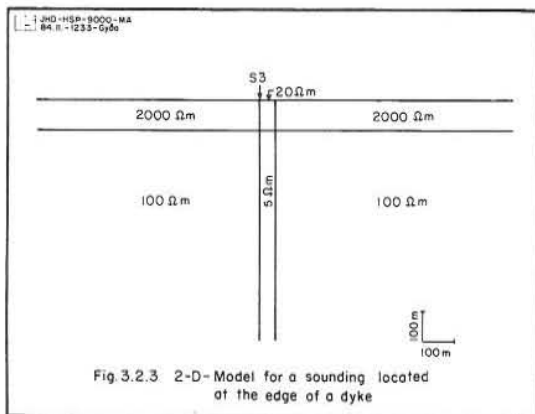


Fig. 3.2.4 Interpretation of a sounding located at the edge of the conductive dyke.

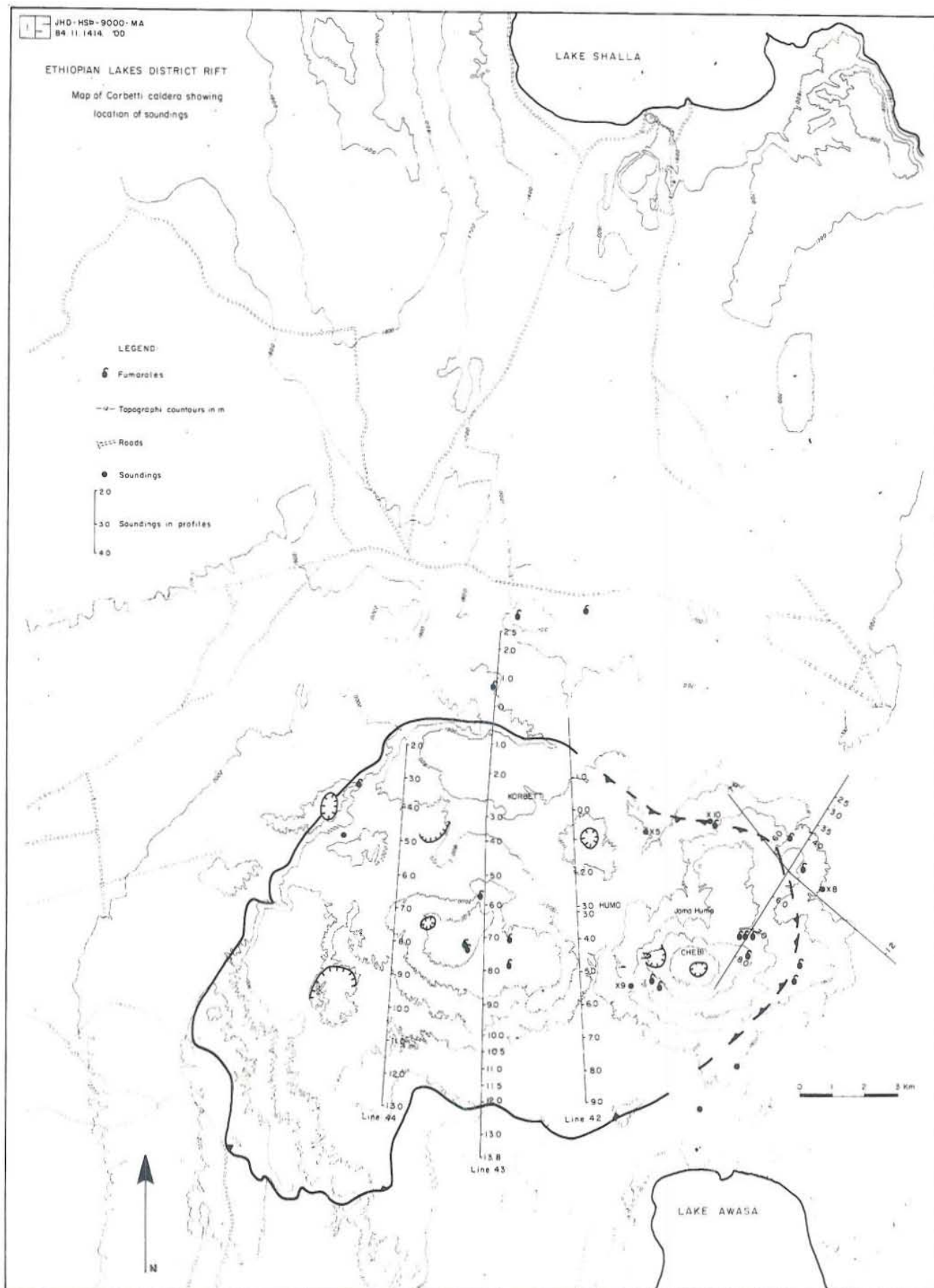


Fig. 4.4.1 Map of Corbetti caldera showing the location of the Schlumberger sounding stations.



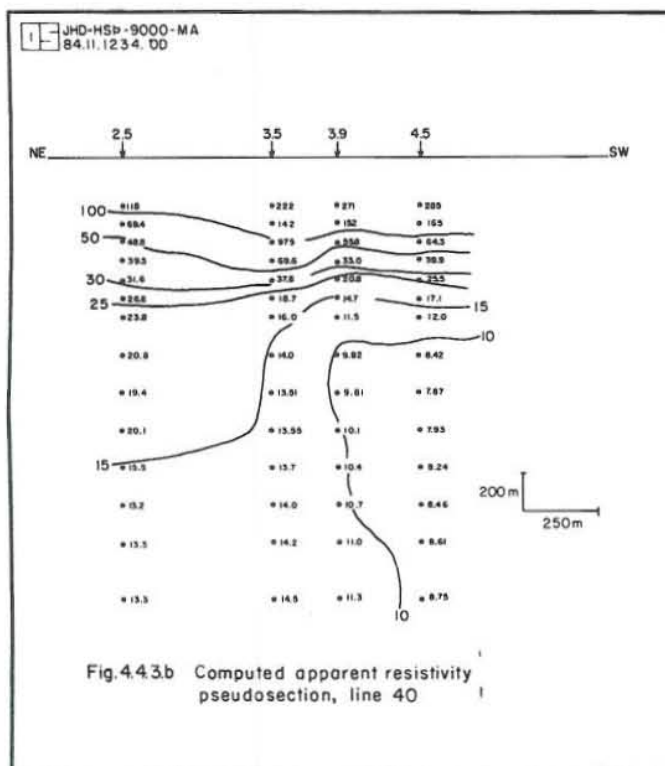
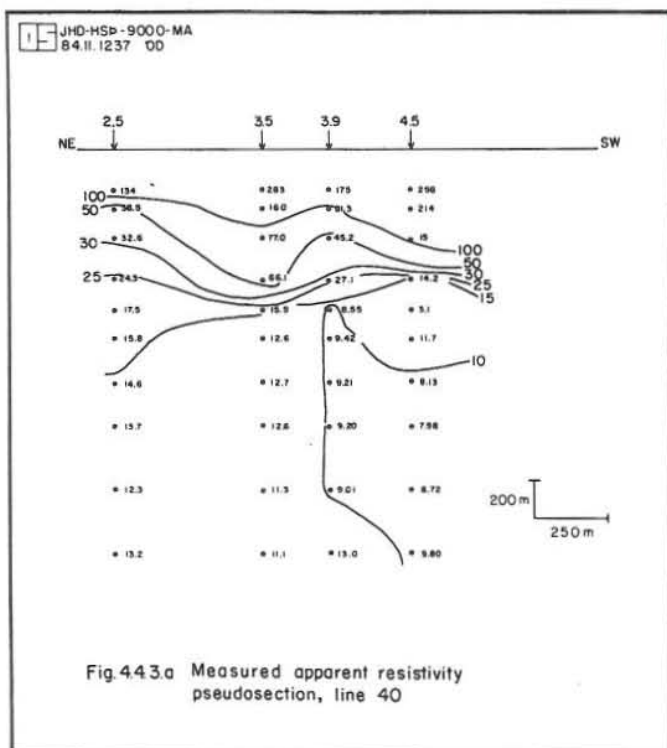
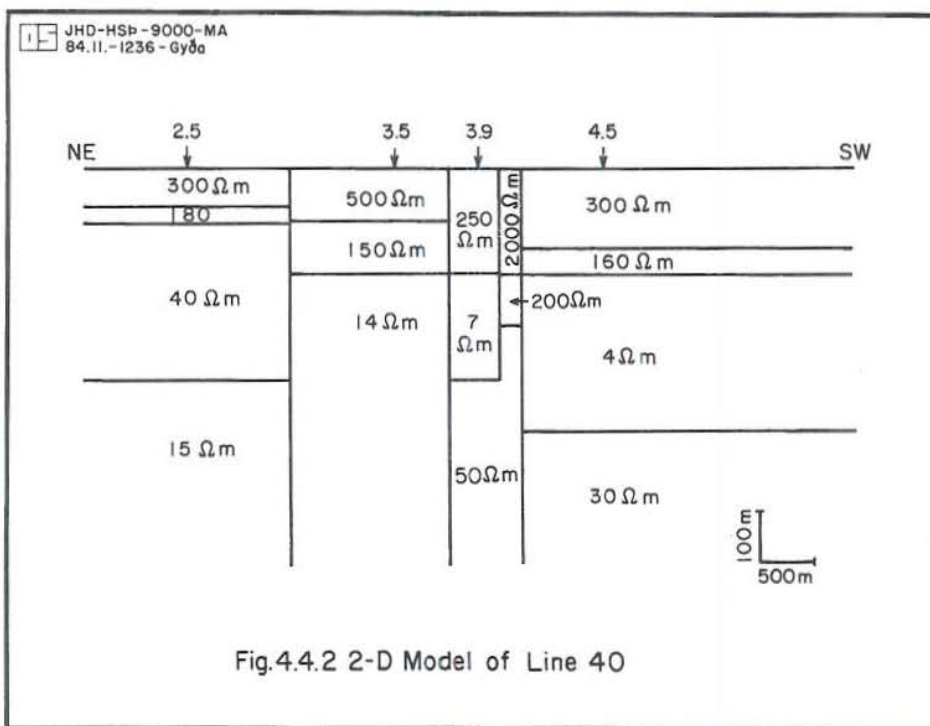
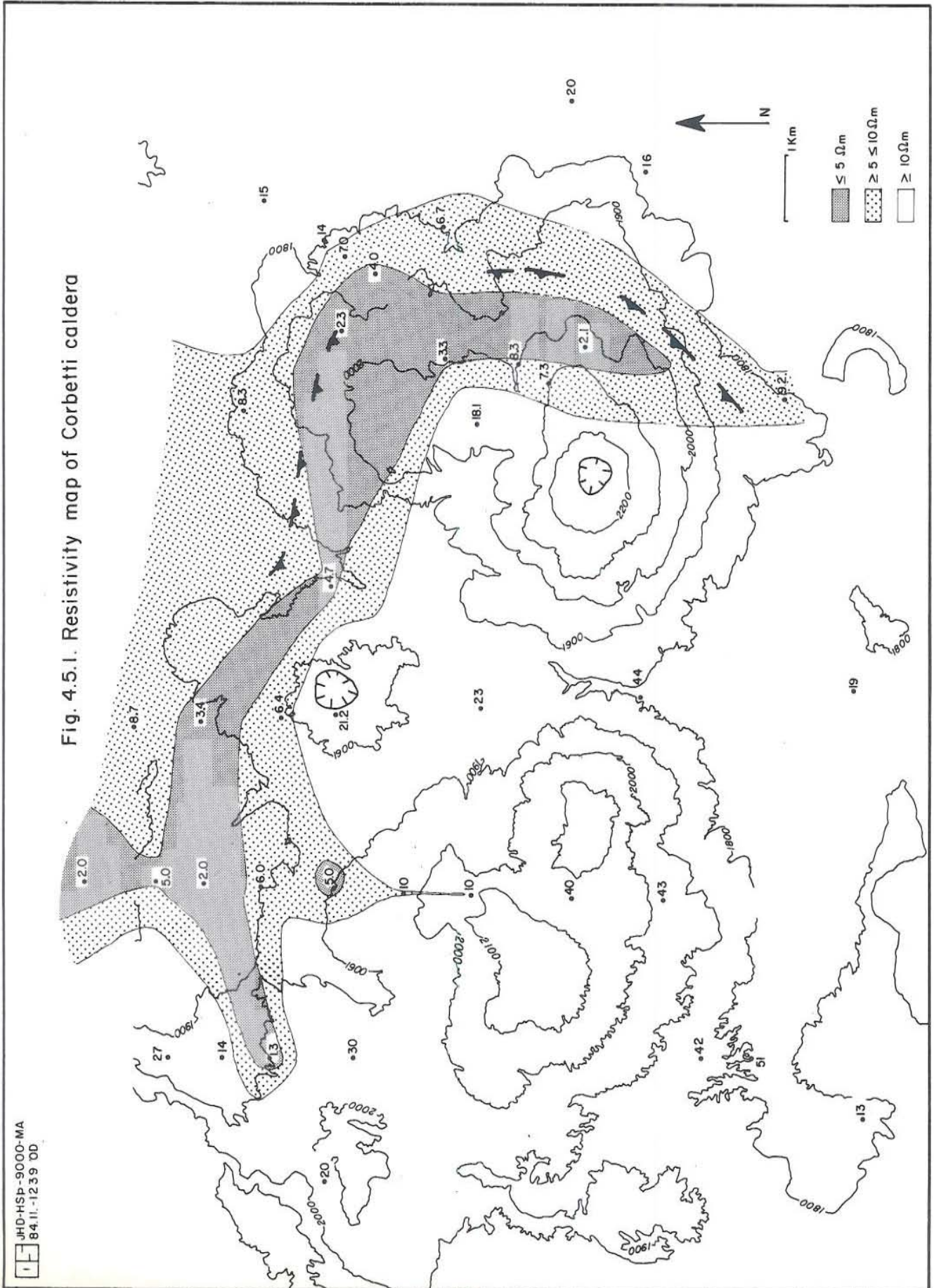
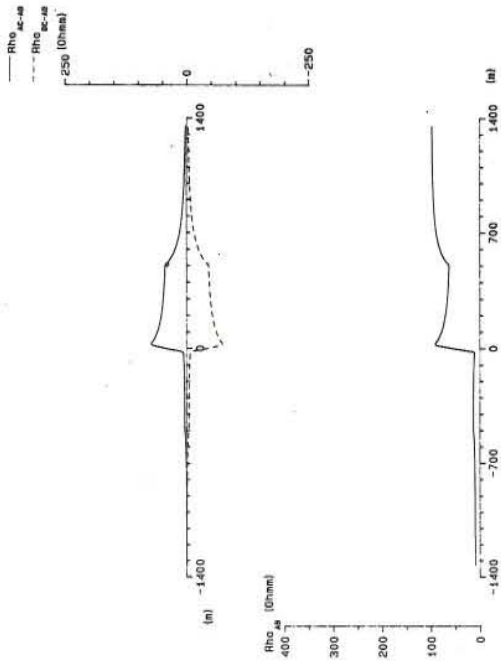




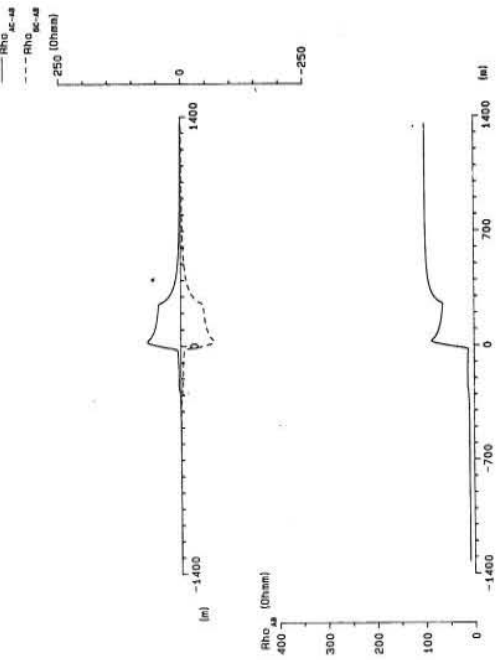
Fig. 4.5.1. Resistivity map of Corbetti caldera



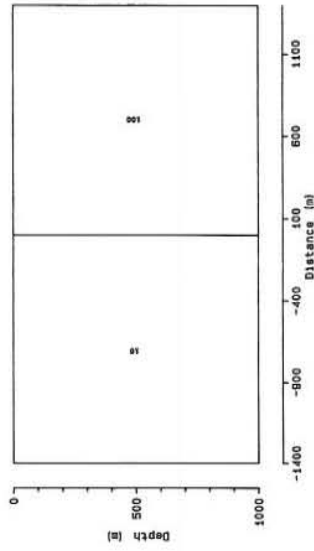
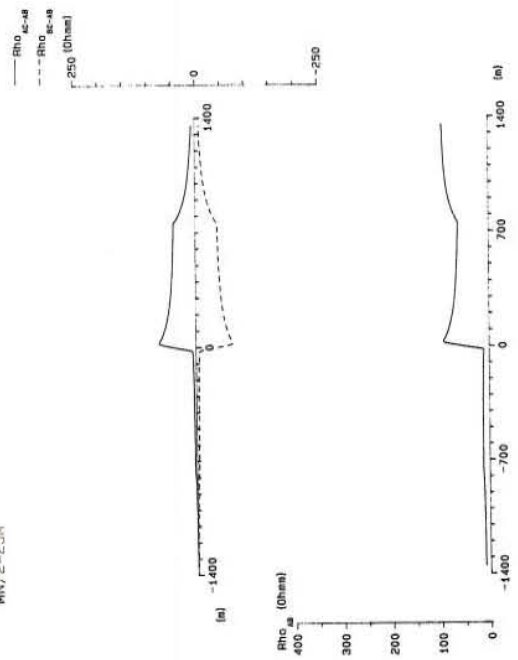

 980152-9000-MA  
 AB/2=500M  
 MN/2=25M




 980152-9000-MA  
 AB/2=250M  
 MN/2=25M




 980152-9000-MA  
 AB/2=750M  
 MN/2=25M




 980152-9000-MA

Fig. 5.4.1 Head-on profiling over a vertical contact.

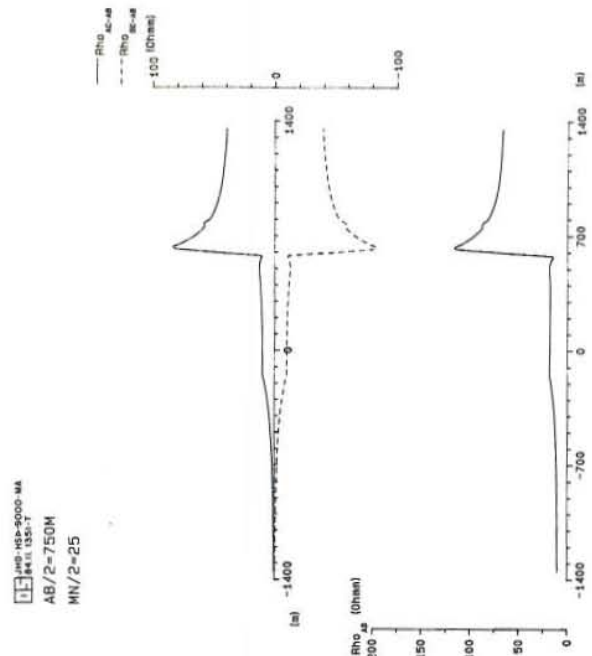
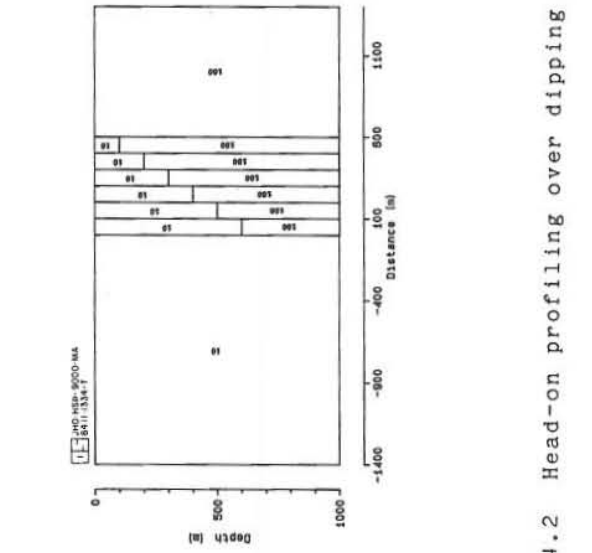
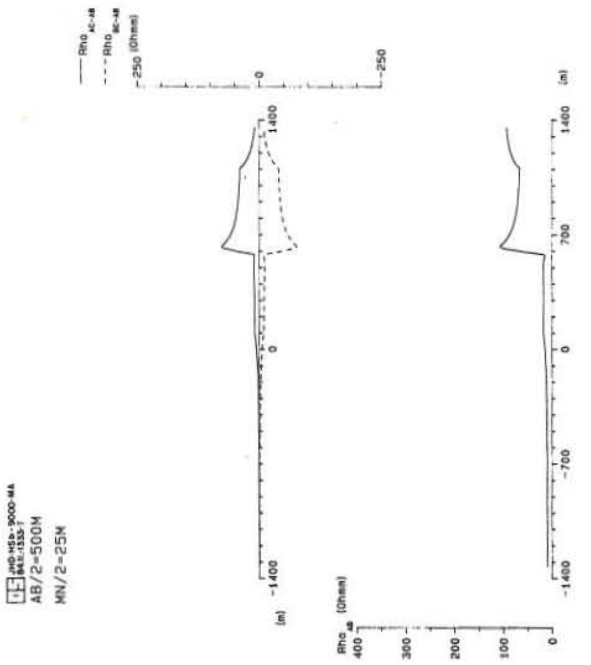
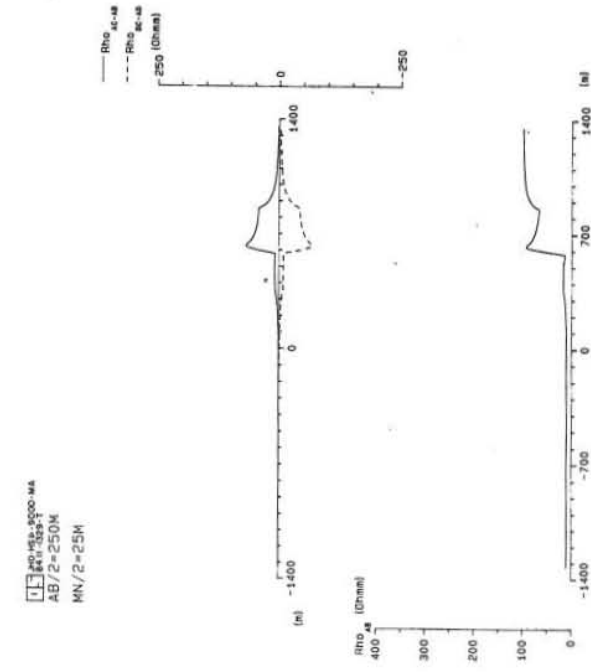


Fig. 5.4.2 Head-on profiling over dipping contacts.

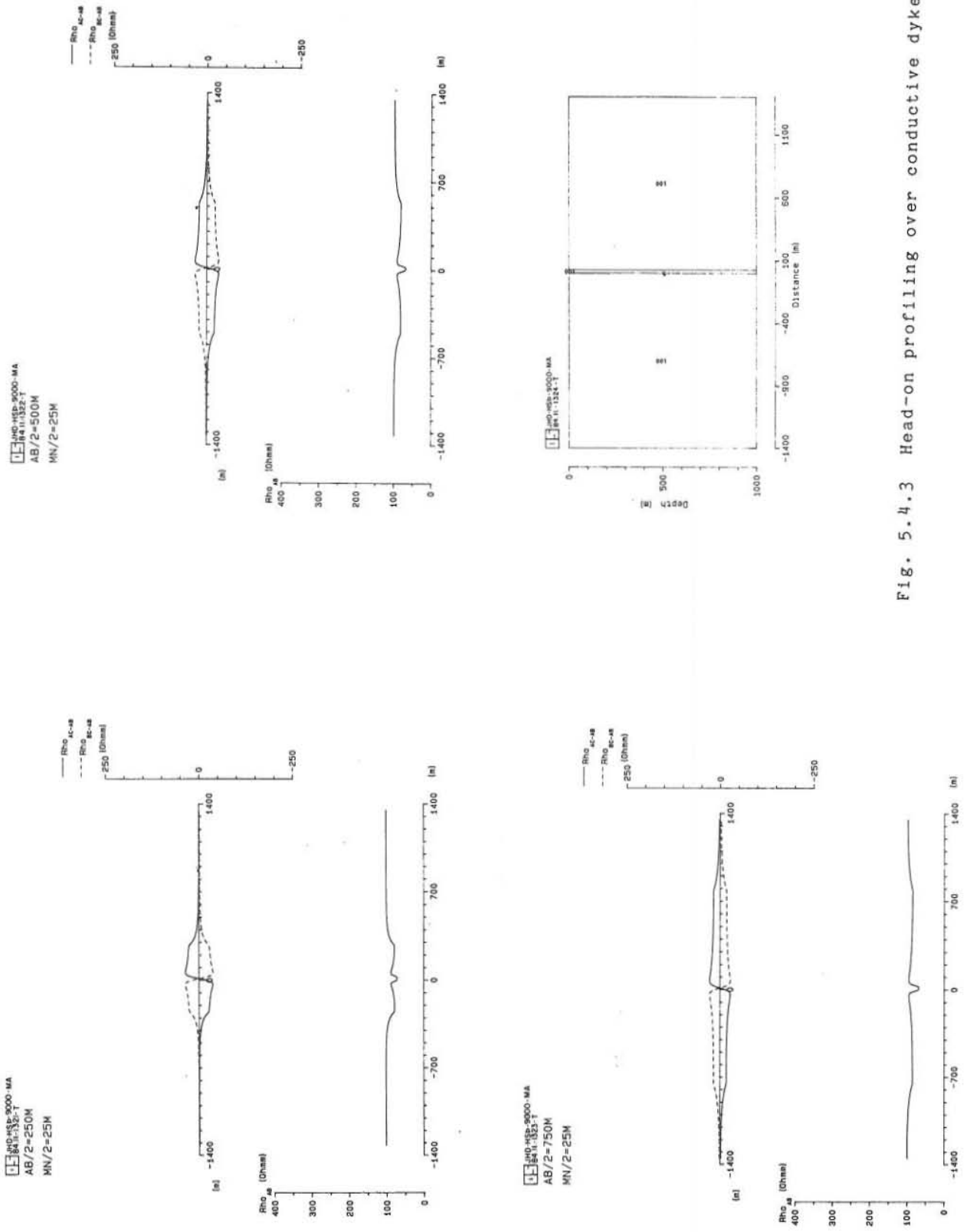
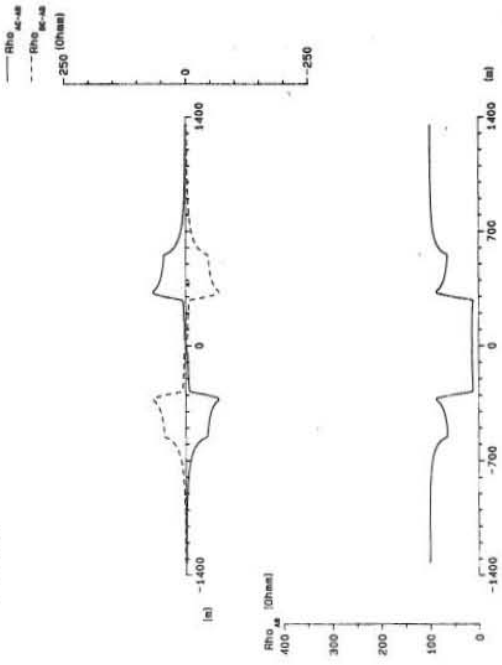
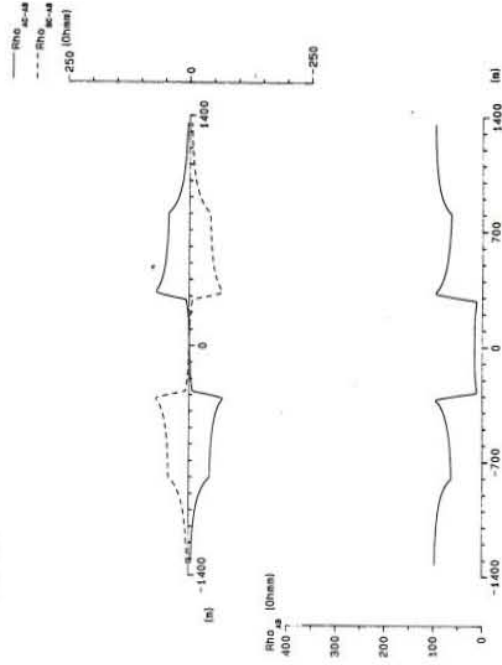



Fig. 5.4.3 Head-on profiling over conductive dyke.

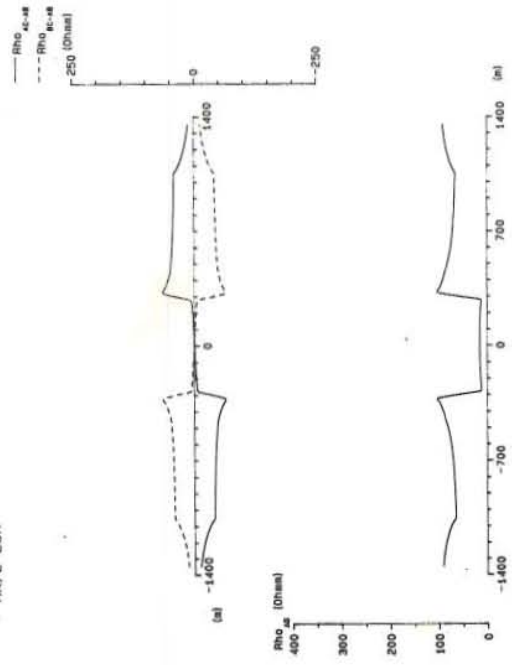

 NOVELS-2000-MA  
 AB/2=250M  
 MN/2=25M




 NOVELS-2000-MA  
 AB/2=500M  
 MN/2=25M




 NOVELS-2000-MA  
 AB/2=750M  
 MN/2=25M




 NOVELS-2000-MA  
 AB/2=500M

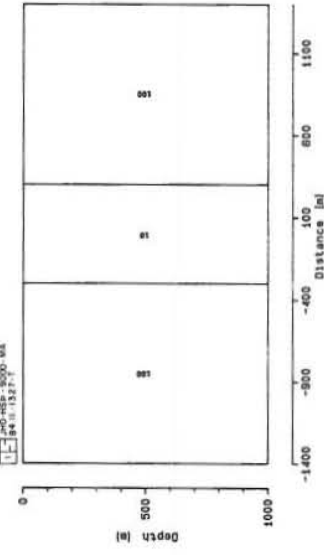


Fig. 5.4.4 Head-on profiling over conductive vertical block.

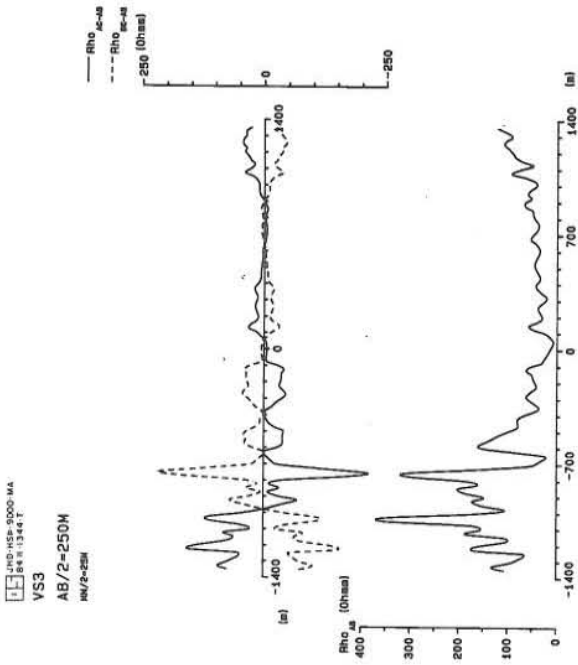
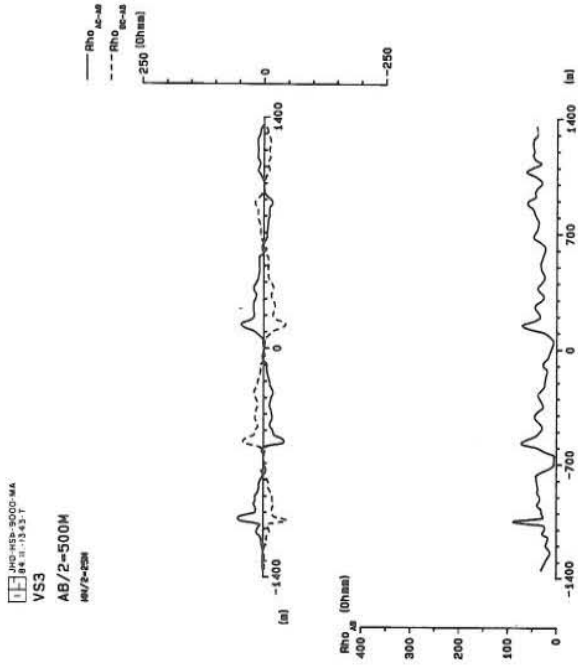


Fig. 5.5.1 Measured head on curves from Krafla (VS3).

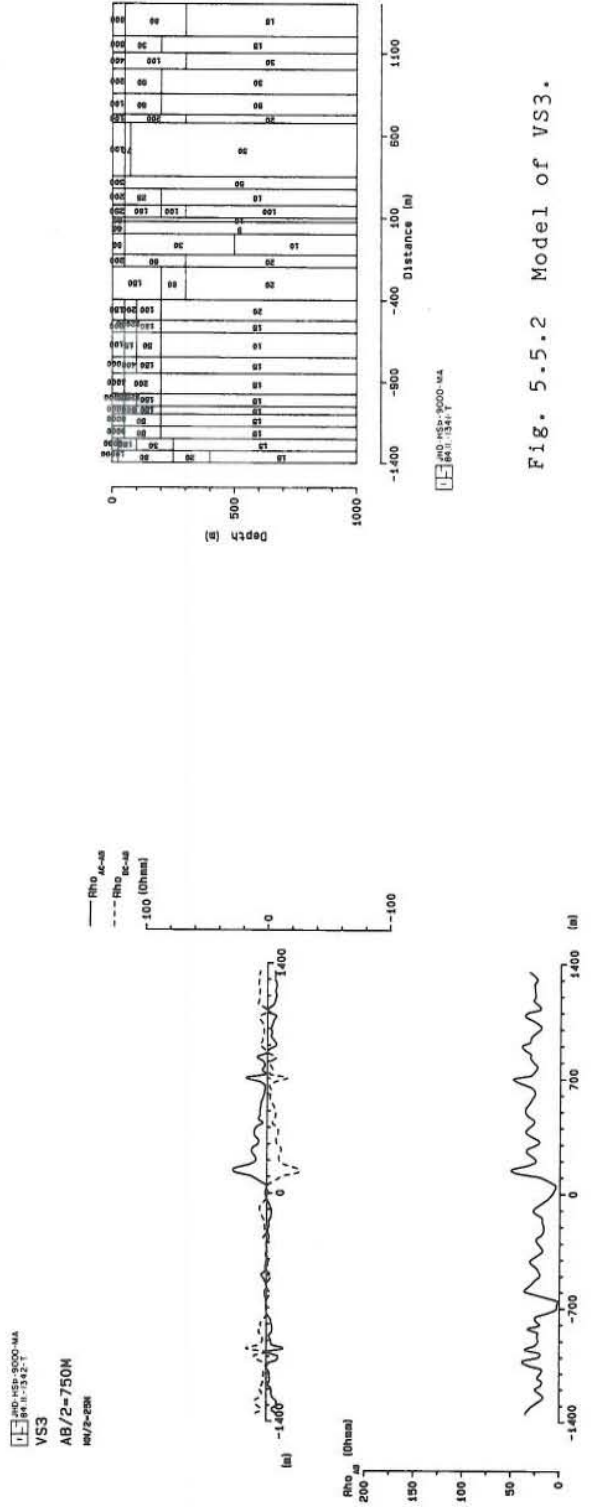


Fig. 5.5.2 Model of VS3.



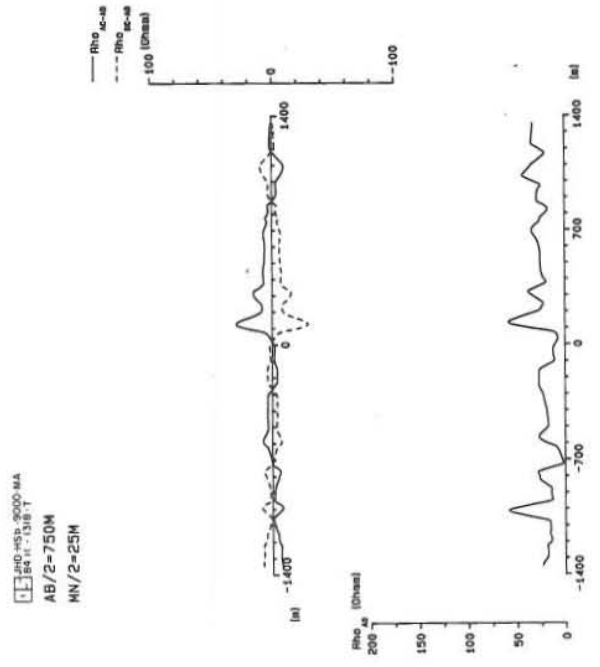
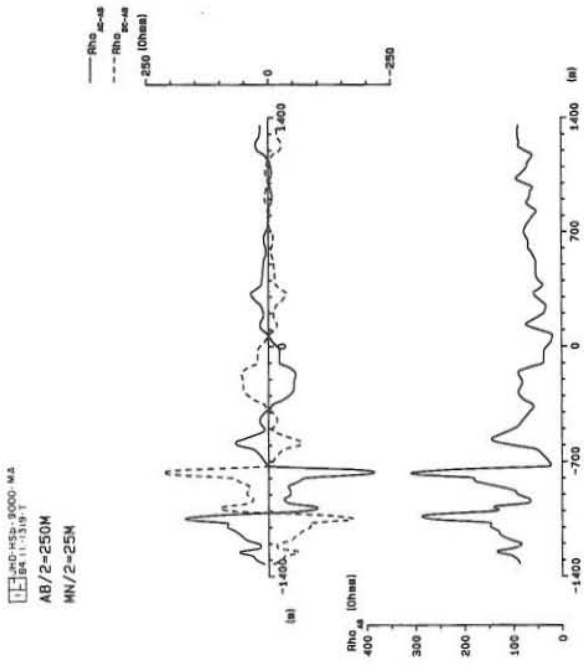
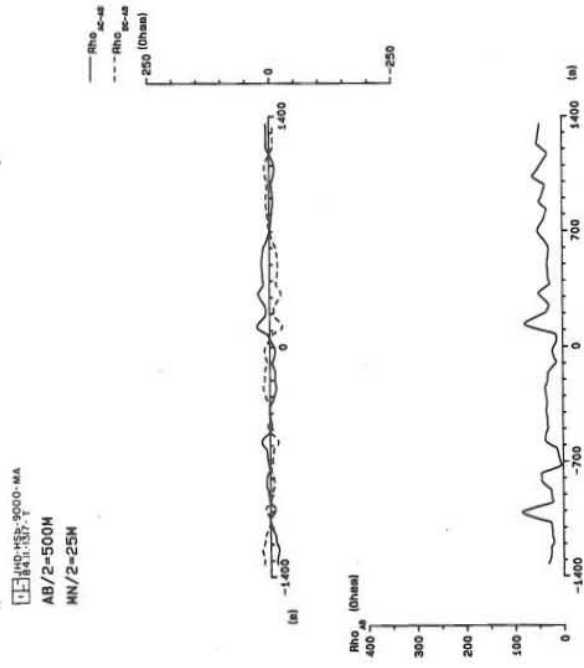


Fig. 5.5.3 Computed curves of the model VS3.

APPENDIX I

